Editors' Suggestion Featured in Physics

Negative Refraction in Time-Varying Strongly Coupled Plasmonic-Antenna–Epsilon-Near-Zero Systems

V. Bruno,[1,*] C. DeVault,[2,3,*] S. Vezzoli,[4,*] Z. Kudyshev,[2,3] T. Huq,[4] S. Mignuzzi,[4] A. Jacassi,[4] S. Saha,[2,3] Y. D. Shah,[1] S. A. Maier,[4,7] D. R. S. Cumming,[6] A. Boltasseva,[2,3] M. Ferrera,[5] M. Clerici,[6] D. Faccio,[1,†] R. Sapienza,[4,‡] and V. M. Shalaev[2,3,§]

[1]*School of Physics and Astronomy, University of Glasgow, G12 8QQ Glasgow, United Kingdom*
[2]*Purdue Quantum Science and Engineering Institute, Purdue University 1205 West State Street, West Lafayette, Indiana 47907, USA*
[3]*School of Electrical and Computer Engineering and Birck Nanotechnology Center, Purdue University, 1205 West State Street, West Lafayette, Indiana 47907, USA*
[4]*The Blackett Laboratory, Department of Physics, Imperial College London, London SW7 2BW, United Kingdom*
[5]*Institute of Photonics and Quantum Sciences, Heriot-Watt University, EH14 4AS Edinburgh, United Kingdom*
[6]*School of Engineering, University of Glasgow, G12 8LT Glasgow, United Kingdom*
[7]*Chair in Hybrid Nanosystems, Nanoinstitute Munich, Faculty of Physics, Ludwig-Maxilimians-Universitat München, 80539 München, Germany*

(Received 9 August 2019; published 30 January 2020)

Time-varying metasurfaces are emerging as a powerful instrument for the dynamical control of the electromagnetic properties of a propagating wave. Here we demonstrate an efficient time-varying metasurface based on plasmonic nano-antennas strongly coupled to an epsilon-near-zero (ENZ) deeply subwavelength film. The plasmonic resonance of the metal resonators strongly interacts with the optical ENZ modes, providing a Rabi level spitting of ~30%. Optical pumping at frequency ω induces a nonlinear polarization oscillating at 2ω responsible for an efficient generation of a phase conjugate and a negative refracted beam with a conversion efficiency that is more than 4 orders of magnitude greater compared to the bare ENZ film. The introduction of a strongly coupled plasmonic system therefore provides a simple and effective route towards the implementation of ENZ physics at the nanoscale.

DOI: 10.1103/PhysRevLett.124.043902

Introduction.—Time-varying systems and metasurfaces are of interest in view of the fundamental physics questions that have arisen [1–7] and also in view of the potential applications ranging from perfect lenses to spectral and temporal shaping of light fields [8–20]. Recent results have shown that thin films of epsilon-near-zero (ENZ) materials with a dielectric permittivity close to zero [21] at optical wavelengths in the visible or near-infrared spectral regions are promising candidates to achieve rapid (on the optical wave oscillation timescale) temporal changes of the optical properties [7]. The very large order-of-unity refractive index changes that can be induced optically [22–25] make it possible to achieve efficient temporal modulation uniformly across the medium [10,26] even in deeply subwavelength thin films [27–29], resulting in optically induced negative refraction with unity efficiency [7]. However, the results demonstrated so far rely on high-intensity optical pumping of the ENZ film in order to achieve such large changes in the refractive index. Recently, the combination of ENZ films with plasmonic structures has led to a significant reduction of the required optical powers for the Kerr nonlinear contribution to the refractive index [30]. We also briefly mention that through an engineered phase gradient discontinuity at the interface between two media, it is possible to achieve anomalous reflection and refraction, including negative refraction without using optical nonlinearities [31].

Coupling between light and matter can be enhanced when two resonant systems with the same optical resonant frequency are brought into close contact [32]. Strong coupling occurs when the strength of the coupling mechanism (measured by the splitting of the two resonant frequencies [33]) dominates the intrinsic losses in the system thus resulting in a double peaked structure in the absorption spectrum or, equivalently, in two well-separated polariton branches in the spectral domain. In the temporal domain, this will give rise to Rabi oscillations between the populations on these two branches and the combination of light-matter states where the matter component can contain a large fraction of the total energy. Strong coupling has been observed in a variety of systems [32,34], ranging from single atoms in cavity [35], quantum dots in photonic crystal [36] to Bose-Einstein condensates [37] and superfluids [38].

Strong coupling at room temperature has also been reported between plasmonic resonators and deeply subwavelength ENZ films [39–43]. In this strongly coupled system, the fundamental plasmonic resonance of a metal antenna resonator is coupled to optical modes supported by the deeply subwavelength ENZ thin film at the frequency where the real part of the dielectric permittivity crosses zero, called the ENZ modes. The ENZ modes can be seen as long-range surface waves which arise from the interaction of two surface plasmon polaritons (SPPs) at the two interfaces of the thin film [28,44–48]. These ENZ modes exhibit a large density of states and can homogeneously confine the electromagnetic radiation within the ENZ [45,49]. Because of the impedance mismatch at the interface between air and the ENZ medium, excitation of the ENZ optical modes is inefficient, while adding strongly coupled antennas enables high electromagnetic fields inside the ENZ film, resulting in enhanced nonlinear responses.

Here, we study optically induced negative refraction from a time-varying, strongly coupled ENZ metasurface based on gold nano-antennas on top of a deeply subwavelength ENZ film. Our experiments show that strongly coupled plasmonic antenna-ENZ systems can be temporally modulated with an optical pump beam through a $\chi^{(3)}$-mediated process. Optical pumping at frequency ω induces a nonlinearity-mediated oscillation at frequency 2ω, which leads to the generation of a phase conjugate (PC) and a negative refracted (NR) beam [8,9]. Experiments were performed by optically pumping at normal incidence a metasurface composed of rectangular metallic nano-antennas on a 40-nm-thick ENZ film and probing the resulting oscillating metasurface with a probe beam incident at a small angle. The generation efficiency of NR and PC waves can provide a quantitative estimate of the strong coupling between the ENZ and the antenna modes, resulting in efficient optically induced temporal variations of the material properties across a broad bandwidth (1200–1700 nm). The optically induced temporal modulation [8,9] and resulting negative refraction and phase conjugation of the input probe beam generated in the strong-coupling regime are four orders of magnitude larger and cover a bandwidth that is 3 times broader in the ENZ wavelength region when compared to the bare ENZ film.

Metasurface properties.—Figure 1(a) shows the real and imaginary parts of the dielectric permittivity via ellipsometry measurements of the 40 nm ITO film on a 1-mm-thick SiO_2 substrate. The ITO film exhibits a zero crossing of the real part at 1400 nm (ENZ wavelength). Figure 1(b) is an example SEM image of the metasurface (top view) showing the geometry of the gold antennas deposited on the ITO surface with length L and periodicity p (see Supplemental Material [50]). The length of the antennas is such that their plasmonic resonance crosses the ENZ wavelength of the ITO film and the periodicity $p \sim 600$–800 nm of the square lattice was chosen so as to maximize the density of the antennas while avoiding antenna-to-antenna coupling.

Figures 1(c) and 1(d) show the numerically simulated (FDTD) and measured transmission spectra around the ENZ wavelength. For an incident optical beam normal to the metasurface and polarized along the long axis of the antenna, the spectra show two resonances corresponding to the two polariton branches of the strongly coupled metasurface. The experimental spectral splitting of the two polariton branches measured at the ENZ wavelength, λ_{ENZ} (i.e., where the ENZ and antenna mode dispersion branches cross) is $\Delta\lambda \sim 420$ nm corresponding to a strong coupling efficiency $\Delta\lambda/\lambda_{\text{ENZ}}$ of ~30% [41,45].

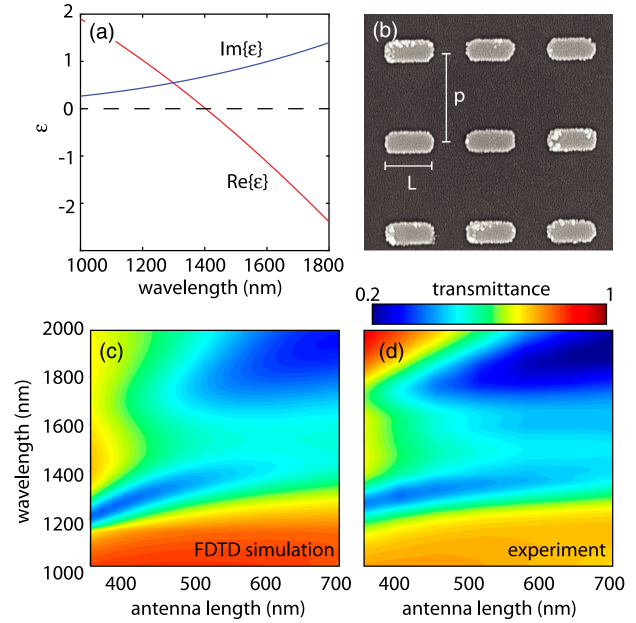

FIG. 1. Linear properties. (a) Dielectric permittivity (ε) for the ITO layer based on a Drude model with real part Re{ε} and imaginary part Im{ε}. (b) SEM image of the square lattice antenna pattern on ITO film (gold antenna length $L = 460$ nm, with period $p = 800$ nm on a $d = 40$ nm thick ITO film). (c) FDTD calculations of linear transmission through the metasurface using the ITO dielectric permittivity in (a). (d) Experimentally measured linear transmission of the metasurface (linear interpolation of measurements performed for antenna lengths of 400, 450, 500, 600, and 650 nm, $p = 800$ nm).

In Fig. 2(a) we report the normalized energy density, calculated from finite difference time domain (FDTD) simulations as the $|E|^2$-field distribution normalized to the input $|E|^2$ distribution at 1400 nm wavelength for the metasurface ($L = 460$ nm and $p = 800$ nm) upon normal incidence of the pump beam. Figure 2(b) shows the normalized energy density along the vertical line [white dashed line in (a)]. For a 1400 nm laser pulse polarized parallel to the long axis of the antenna and at normal incidence, the field intensity is enhanced by a factor greater than 50 with respect to the bare ITO. In Fig. 2(c) we plot the wavelength dependence of the energy density across the full bandwidth covering the two polariton branches calculated at two different points indicated as "1" and "2" in Fig. 2(a), showing an enhancement that is 40 times greater with respect to the bare ITO layer over a ~300 nm bandwidth.

Experiments.—By using a pump and probe setup, we perform a degenerate four wave mixing (FWM) experiment

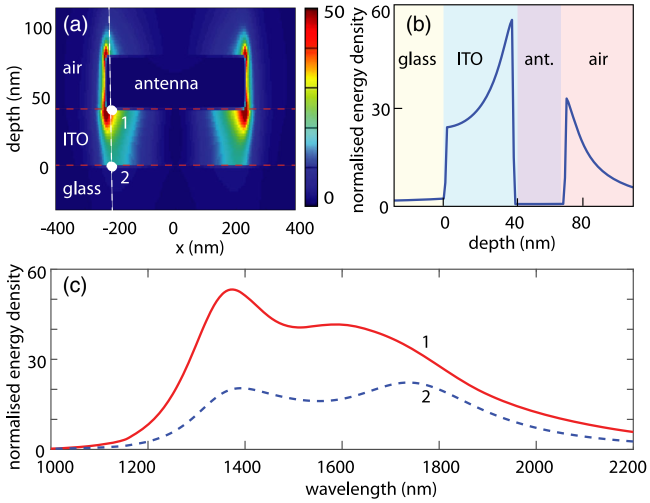

FIG. 2. FDTD simulation of the normalized energy density (calculated as the $|E|^2$-field distribution normalized to the input $|E|^2$) in (a) for the 2D nano-antenna pattern on top of a 40 nm layer of ITO. (b) Depth profile of the normalized energy density across the metasurface [dashed white line in (a)]. (c) The normalized energy density versus wavelength calculated at the two points indicated with "1" and "2" in (a).

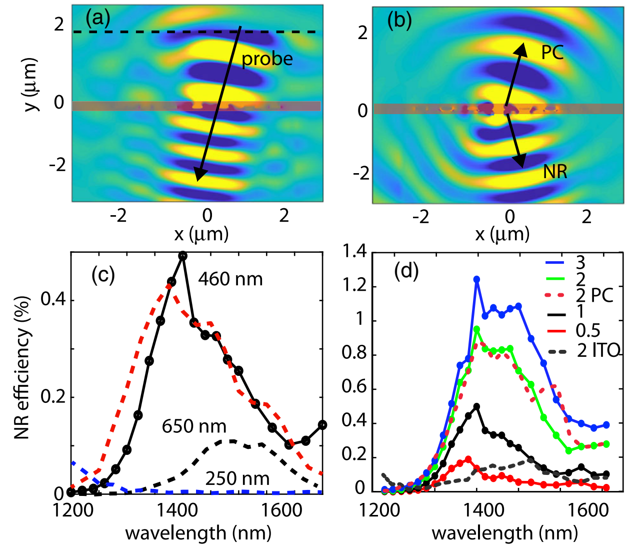

FIG. 3. Simulations and experiments. (a) Nonlinear FDTD simulation of input probe beam. The arrow indicates the probe direction (pump not shown), the red shaded area shows the metasurface area, and the dashed line indicates the location of the E-field source. (b) Phase conjugated and negative refracted beams are generated at the metasurface. (c) NR efficiency (NR energy normalized to input probe energy, expressed in percent) simulated with a nonlinear FDTD based on the same material and geometry as those used in the experiments (dashed red line) and antenna length $L = 460$ nm (indicated in the graph). Also shown (solid-black curve) is the measured curve for 1 $\mathrm{GW/cm^2}$. The blue and black dashed lines show the simulated NR efficiency with plasmonic antennas with longer or shorter lengths (250 and 650 nm, indicated in the graph) so as to be detuned from the ENZ wavelength. The NR efficiency drops by nearly an order of magnitude thus highlighting the role played by strong coupling in the FWM enhancement. (d) The measured negative refraction (and an example of PC) signal efficiency for antennas on a film of 40 nm of ITO (antenna length $L = 460$ nm, period $p = 800$ nm) for various pump powers indicated in the graph legend in $\mathrm{GW/cm^2}$. The NR efficiency of the bare ITO film for a pump power of 2 $\mathrm{GW/cm^2}$, multiplied by 1000 is shown for reference (dashed black curve).

(i.e., a single pump beam and a single probe beam, both at the same wavelength) in the 1180 to 1710 nm spectral range. The optical pump beam has normal incidence on the sample, while the probe is incident at a small (6°) angle. The two incident laser pulses are copolarized (parallel to the long axis of the antenna) and have a temporal duration of 240 fs, the same central wavelength, and 100 kHz repetition rate. The generated NR and PC are measured with a photodiode and compared to the transmission of the bare ITO in order to evaluate the efficiency of the nonlinear process. In Fig. 3 we show a comparison of the experimental results to a nonlinear FDTD simulation reproducing the experiment conditions (antenna length $L = 460$ nm and $p = 800$ nm). The linear properties of the ITO film are based on the experimental measurements shown in Fig. 1(a), while the nonlinear response is described via the third order nonlinear susceptibility $\chi^{(3)} = 9 \times 10^{-18}\ \mathrm{m^2/V^2}$ [53]. In these simulations, we blueshift the central wavelength of the probe by 100 nm from the pump in order to discriminate the output NR and PC fields. Figures 3(a) and 3(b) show the simulated near field distribution for the incident probe and the generated NR and PC fields. The simulated NR efficiency (i.e., the NR efficiency normalized to the input probe energy, expressed in percent) is shown for a pump intensity of 1 $\mathrm{GW/cm^2}$ in Fig. 3(c) (red dashed curve) and matches well to the raw experimental data (black curve). Figure 3(c) also shows the same FDTD simulations with detuned plasmonic antennas (i.e., antenna lengths of 250 and 650 nm) so as to be out of the strong coupling regime. The FWM efficiency drops in both cases by an order of magnitude, providing strong evidence that strong coupling is enhancing the nonlinear process.

In Fig. 3(d) we show the measured NR signal efficiency for various pump powers indicated in the graph in $\mathrm{GW/cm^2}$. The dotted black curve shows for comparison the NR efficiency at 2 $\mathrm{GW/cm^2}$ pump power for the bare ITO film, multiplied by 1000. We see that the measured FWM efficiency of the metasurface is enhanced by more than 4 orders of magnitude when compared to the bare ITO. The absolute efficiency of both the NR and PC (one example shown, red-dotted line) nonlinear processes is of order ∼1% over a very large bandwidth of ∼300 nm. Both the NR and PC exhibit the same trend, as expected for a deeply subwavelength film that is uniformly modulated at twice the probe beam frequency [9]. To verify the FWM process is primarily due to the strong coupling between the gold antennas and ITO film, and is not due solely to the gold nonlinearity, we repeated all experiments for the gold antennas deposited on a glass substrate. We find the gold antennas alone do not produce a detectable signal at the same pump powers.

Model and data analysis.—In order to further understand the nonlinear enhancement, we model the pump-probe interaction in the metasurface as a FWM process in which the 4 orders of magnitude enhancement of the negative refraction and phase conjugation processes emerge as a result of the increased optical energy density in the ENZ layer. Indeed, in the strongly coupled system the E field of both pump and probe is strongly enhanced inside the ITO layer as the plasmonic antennas convert the incident propagating waves into waves localized in their near field. We model the nonlinear generation of beams in a FWM process starting from the numerically simulated distribution of linear fields, as described, for instance, in Ref. [54]. FWM is driven by a nonlinear polarization in the ITO layer, $P \propto E_p^2 E_s^*$, where E_p is the pump field, E_s the probe field, and P is the microscopic source of the measured fields of the NR and PC beams. By making use of the reciprocity theorem, one can calculate the expected FWM E field generated by P as

$$E(\omega) \propto \int \varepsilon_0 \chi^{(3)}(\omega) \vdots \mathbf{E}_p^2(\omega)\mathbf{E}_s^*(\omega) \cdot \mathbf{E}_{\rm det}(\omega) dV, \quad (1)$$

where the integral is calculated over the ITO volume and $E_{\rm det}$ is the field inside the ENZ film generated by a point source representing the detector in the far field (see Supplemental Material [50]). The $\vdots$ indicates a triple scalar tensor product between $\chi^{(3)}$ and the three fields interacting in the nonlinear medium. The FWM efficiency, measured in the experiment as the ratio between the energy radiated into NR (or PC) and the incident probe energy and is thus proportional to $|E|^2$. This is true both for the bare ITO and the metasurface. Taking the ratio between the efficiency, $\eta_{\rm metasurface}$, of NR for the metasurface and the efficiency, $\eta_{\rm ITO}$, of NR for bare ITO removes the spectral dependence of the nonlinear permittivity $\chi^{(3)}$, of the linear permittivity, the sample thickness, and all other constants:

$$\eta_{\rm norm}(\omega) = \frac{|E_{\rm metasurface}|^2}{|E_{\rm ITO}|^2}. \quad (2)$$

This relation directly estimates the trend of the normalized efficiency of the NR and PC processes from the energy density calculation shown in Fig. 2(c). Figure 4 shows the result, together with the corresponding measured $\eta_{\rm norm}$ based on the experimental data shown in Fig. 3(d) for $p = 800$ nm and an additional periodicity $p = 600$ nm. As can be seen, our model based on the energy density enhancement in the metasurface explains the experimental results for the two different antenna configurations studied in this work, although the longer wavelength peak in the spectrum appears to have higher visibility in the experiments with respect to the theoretical model. Our primary conclusion is that the strong coupling between the plasmonic antennas and ENZ film enhances light-matter interaction and, therefore, increases the conversion efficiency of our time-varying metasurface by a factor greater than 15 000. Such efficient time-varying surfaces can be obtained by optically pumping the metasurface with relatively low and readily accessible optical pumping powers of 0.5 mW, corresponding to peak intensities on the surface of 0.5 GW/cm^2.

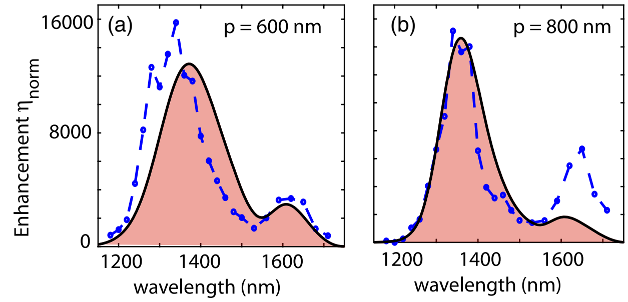

FIG. 4. Theoretical model and measurements. (a) NR efficiency $\eta_{\rm norm}$ as measured for the antenna-ITO coupled system for a pump intensity 0.5 GW/cm^2 and periodicity 600 nm and, (b) for periodicity 800 nm (antenna length is 460 nm in both cases).

Conclusions.—Strongly coupled plasmonic-antenna–ENZ systems exhibit a 15 000-fold enhancement in the negative refraction and phase conjugation signals compared to the bare ENZ films. We have developed a nonlinear model that elucidates the relation between FWM enhancement and the increased energy density inside the ENZ film which arises from strong coupling. Efficient time-varying surfaces with optical pumping at relatively low and readily accessible powers provide a route towards applications in which light is controlled by light in compact, subwavelength devices alongside a means to investigate fundamental physics, potentially including photon pair generation from deeply subwavelength systems.

D. F. acknowledges financial support from EPSRC (UK Grants EP/M009122/1 and EP/P006078/2). M. C. acknowledges the support from the United Kingdom Research and Innovation (UKRI, Innovation Fellowship EP/S001573/1). The Purdue team acknowledges support by the U.S. Department of Energy, Office of Basic Energy Sciences, Division of Materials Sciences and Engineering under Award No. DE-SC0017717 (sample characterization), Air Force Office of Scientific Research (AFOSR) Award No. FA9550-18-1-0002 (numerical modeling), and Office of Naval Research Award (nonlinear optical characterization). S. V., S. M., A. J., S. A. M., and R. S. acknowledge funding by EPSRC (EP/P033431 and EP/M013812). S. A. M. acknowledges the Lee-Lucas Chair in Physics and the DFG Cluster of

Excellence Nanoscience Initiative Munich (NIM). T. H. acknowledges the Schrödinger Scholarship. Data relevant to this work are available for download at Ref. [55].

*These authors contributed equally to this work.
†daniele.faccio@glasgow.ac.uk
‡r.sapienza@imperial.ac.uk
§shalaev@purdue.edu

[1] J. T. Mendonça, *Theory of Photon Acceleration* (CRC Press, Boca Raton, 2000).
[2] P. D. Nation, J. R. Johansson, M. P. Blencowe, and F. Nori, Rev. Mod. Phys. **84**, 1 (2012).
[3] E. Yablonovitch, Phys. Rev. Lett. **62**, 1742 (1989).
[4] N. Westerberg, S. Cacciatori, F. Belgiorno, F. Dalla Piazza, and D. Faccio, New J. Phys. **16**, 075003 (2014).
[5] A. Prain, S. Vezzoli, N. Westerberg, T. Roger, and D. Faccio, Phys. Rev. Lett. **118**, 133904 (2017).
[6] V. Bacot, M. Labousse, A. Eddi, M. Fink, and E. Fort, Nat. Phys. **12**, 972 (2016).
[7] S. Vezzoli, V. Bruno, C. DeVault, T. Roger, V. M. Shalaev, A. Boltasseva, M. Ferrera, M. Clerici, A. Dubietis, and D. Faccio, Phys. Rev. Lett. **120**, 043902 (2018).
[8] S. Maslovski and S. Tretyakov, J. Appl. Phys. **94**, 4241 (2003).
[9] J. Pendry, Science **322**, 71 (2008).
[10] A. Shaltout, A. Kildishev, and V. Shalaev, Opt. Mater. Express **5**, 2459 (2015).
[11] D. L. Sounas and A. Alù, Nat. Photonics **11**, 774 (2017).
[12] A. M. Shaltout, V. M. Shalaev, and M. L. Brongersma, Science **364**, eaat3100 (2019).
[13] G. Sartorello, N. Olivier, J. Zhang, W. Yue, D. J. Gosztola, G. P. Wiederrecht, G. Wurtz, and A. V. Zayats, ACS Photonics **3**, 1517 (2016).
[14] L. H. Nicholls, F. J. Rodríguez-Fortuño, M. E. Nasir, R. M. Córdova-Castro, N. Olivier, G. A. Wurtz, and A. V. Zayats, Nat. Photonics **11**, 628 (2017).
[15] M. Rahmani, G. Leo, I. Brener, A. V. Zayats, S. A. Maier, C. De Angelis, H. Tan, V. F. Gili, F. Karouta, R. Oulton *et al.*, Opto-Electron. Adv. **01**, 180021 (2018).
[16] L. H. Nicholls, T. Stefaniuk, M. E. Nasir, F. J. Rodríguez-Fortuño, G. A. Wurtz, and A. V. Zayats, Nat. Commun. **10**, 2967 (2019).
[17] A. Ciattoni, A. Marini, C. Rizza, and C. Conti, Light Sci. & Appl. **7**, 5 (2018).
[18] T. Šikola, R. Kekatpure, E. Barnard, J. White, P. Van Dorpe, L. Břínek, O. Tomanec, J. Zlámal, D. Lei, Y. Sonnefraud *et al.*, Appl. Phys. Lett. **95**, 253109 (2009).
[19] M. R. Scherbakov *et al.*, Nat. Commun. **10**, 1345 (2019).
[20] Y. Hadad, D. L. Sounas, and A. Alu, Phys. Rev. B **92**, 100304(R) (2015).
[21] I. Liberal and N. Engheta, Nat. Photonics **11**, 149 (2017).
[22] M. Z. Alam, I. De Leon, and R. W. Boyd, Science **352**, 795 (2016).
[23] L. Caspani, R. P. M. Kaipurath, M. Clerici, M. Ferrera, T. Roger, J. Kim, N. Kinsey, M. Pietrzyk, A. Di Falco, V. M. Shalaev, A. Boltasseva, and D. Faccio, Phys. Rev. Lett. **116**, 233901 (2016).
[24] M. Clerici, N. Kinsey, C. DeVault, J. Kim, E. G. Carnemolla, L. Caspani, A. Shaltout, D. Faccio, V. Shalaev, A. Boltasseva *et al.*, Nat. Commun. **8**, 15829 (2017).
[25] E. G. Carnemolla, L. Caspani, C. DeVault, M. Clerici, S. Vezzoli, V. Bruno, V. M. Shalaev, D. Faccio, A. Boltasseva, and M. Ferrera, Opt. Mater. Express **8**, 3392 (2018).
[26] A. Marini and F. G. De Abajo, Sci. Rep. **6**, 20088 (2016).
[27] A. Capretti, Y. Wang, N. Engheta, and L. Dal Negro, ACS Photonics **2**, 1584 (2015).
[28] T. S. Luk, D. De Ceglia, S. Liu, G. A. Keeler, R. P. Prasankumar, M. A. Vincenti, M. Scalora, M. B. Sinclair, and S. Campione, Appl. Phys. Lett. **106**, 151103 (2015).
[29] A. Capretti, Y. Wang, N. Engheta, and L. Dal Negro, Opt. Lett. **40**, 1500 (2015).
[30] M. Z. Alam, S. A. Schulz, J. Upham, I. De Leon, and R. W. Boyd, Nat. Photonics **12**, 79 (2018).
[31] X. Ni, N. K. Emani, A. V. Kildishev, A. Boltasseva, and V. M. Shalaev, Science **335**, 427 (2012).
[32] P. Törmä and W. L. Barnes, Rep. Prog. Phys. **78**, 013901 (2015).
[33] S. De Liberato, C. Ciuti, and I. Carusotto, Phys. Rev. Lett. **98**, 103602 (2007).
[34] A. Benz, S. Campione, S. Liu, I. Montano, J. Klem, A. Allerman, J. Wendt, M. Sinclair, F. Capolino, and I. Brener, Nat. Commun. **4**, 2882 (2013).
[35] R. J. Thompson, G. Rempe, and H. J. Kimble, Phys. Rev. Lett. **68**, 1132 (1992).
[36] T. Yoshie, A. Scherer, J. Hendrickson, G. Khitrova, H. Gibbs, G. Rupper, C. Ell, O. Shchekin, and D. Deppe, Nature (London) **432**, 200 (2004).
[37] J. D. Plumhof, T. Stöferle, L. Mai, U. Scherf, and R. F. Mahrt, Nat. Mater. **13**, 247 (2014).
[38] A. Amo, J. Lefrère, S. Pigeon, C. Adrados, C. Ciuti, I. Carusotto, R. Houdré, E. Giacobino, and A. Bramati, Nat. Phys. **5**, 805 (2009).
[39] Y. C. Jun, J. Reno, T. Ribaudo, E. Shaner, J.-J. Greffet, S. Vassant, F. Marquier, M. Sinclair, and I. Brener, Nano Lett. **13**, 5391 (2013).
[40] S. A. Schulz, A. A. Tahir, M. Z. Alam, J. Upham, I. De Leon, and R. W. Boyd, Phys. Rev. A **93**, 063846 (2016).
[41] S. Campione, J. R. Wendt, G. A. Keeler, and T. S. Luk, ACS Photonics **3**, 293 (2016).
[42] J. R. Hendrickson, S. Vangala, C. Dass, R. Gibson, J. Goldsmith, K. Leedy, D. E. Walker, Jr., J. W. Cleary, W. Kim, and J. Guo, ACS Photonics **5**, 776 (2018).
[43] N. C. Passler, C. R. Gubbin, T. G. Folland, I. Razdolski, D. S. Katzer, D. F. Storm, M. Wolf, S. De Liberato, J. D. Caldwell, and A. Paarmann, Nano Lett. **18**, 4285 (2018).
[44] S. Vassant, A. Archambault, F. Marquier, F. Pardo, U. Gennser, A. Cavanna, J.-L. Pelouard, and J.-J. Greffet, Phys. Rev. Lett. **109**, 237401 (2012).
[45] S. Campione, S. Liu, A. Benz, J. F. Klem, M. B. Sinclair, and I. Brener, Phys. Rev. Applied **4**, 044011 (2015).
[46] S. Campione, I. Kim, D. de Ceglia, G. A. Keeler, and T. S. Luk, Opt. Express **24**, 18782 (2016).

[47] E. L. Runnerstrom, K. P. Kelley, E. Sachet, C. T. Shelton, and J.-P. Maria, ACS Photonics **4**, 1885 (2017).

[48] S. Vassant, J.-P. Hugonin, F. Marquier, and J.-J. Greffet, Opt. Express **20**, 23971 (2012).

[49] A. Ciattoni, A. Marini, C. Rizza, M. Scalora, and F. Biancalana, Phys. Rev. A **87**, 053853 (2013).

[50] See Supplemental Material at http://link.aps.org/supplemental/10.1103/PhysRevLett.124.043902 for the strong coupling evaluation and the model used to extrapolate the FWM efficiency, which includes Refs. [51,52].

[51] J. Kim, A. Dutta, G. V. Naik, A. J. Giles, F. J. Bezares, C. T. Ellis, J. G. Tischler, A. M. Mahmoud, H. Caglayan, O. J. Glembocki *et al.*, Optica **3**, 339 (2016).

[52] C. T. DeVault, V. A. Zenin, A. Pors, K. Chaudhuri, J. Kim, A. Boltasseva, V. M. Shalaev, and S. I. Bozhevolnyi, Optica **5**, 1557 (2018).

[53] J. L. Humphrey and D. Kuciauskas, J. Appl. Phys. **100**, 113123 (2006).

[54] K. O'Brien, H. Suchowski, J. Rho, A. Salandrino, B. Kante, X. Yin, and X. Zhang, Nat. Mater. **14**, 379 (2015).

[55] http://researchdata.gla.ac.uk/id/eprint/903.